The Journal of Neuroscience, May 15, 1997, 17(10):3412–3424

Presynaptic Recordings from *Drosophila*: Correlatin of Macroscopic and Single-Channel K^+ Currents

Manuel Martínez-Padrón and Alberto Ferrús

Instituto Cajal (Consejo Superior de Investigaciones Científicas), 28002 Madrid, Spain

We have performed direct electrophysiological recordings from *Drosophila* peptidergic synaptic boutons *in situ*, taking advantage of a mutation, *ecdysone*, which causes an increase in size of these terminals. Using patch-clamp techniques, we have analyzed voltage-dependent potassium currents at the macroscopic and single-channel level. The synaptic membrane contained at least two distinct voltage-activated potassium currents with different kinetics and voltage sensitivity: an I_A-like current with fast activation and inactivation kinetics and voltage-dependent steady-state inactivation; a complex delayed current that includes a slowly inactivating component, resembling the I_K described in other preparations; and a noninactivating component. The I_A-like current in these peptidergic boutons is not encoded by the gene *Shaker*, because it is not affected by null mutations at this locus. Rather, synaptic I_A has properties similar to those of the *Shal*-encoded I_A. Single-channel recordings revealed the presence in synaptic membranes of three different potassium channel types (A_2, K_D, K_L), with biophysical properties that could account for the macroscopic currents and resemble those of the *Shal*, *Shab*, and *Shaw* channels described in heterologous expression systems and *Drosophila* neuronal somata. A_2 channels (6–9 pS) have brief open times, and like the macroscopic I_A they exhibited voltage-dependent steady-state inactivation and a rapidly inactivating ensemble average current profile. K_D channels (13–16 pS) had longer open times, activate and inactivate with much slower kinetics, and may account for the slowly inactivating component of the macroscopic current. K_L (44–54 pS) channels produced a noninactivating ensemble average and may contribute to the delayed macroscopic current observed.

Key words: Drosophila; *presynaptic terminal; K^+ channels;* Shaker; Shal; Shab; *neuropeptides*

The physiology of the nervous system has its cornerstone in the biology of synaptic terminals. Substantial progress has been made in the molecular characterization of synapses in vertebrates as well as in invertebrates (Bennett and Scheller, 1994; Jahn and Sudhof, 1994; Schwarz, 1994; Littleton and Bellen, 1995). An understanding of the function of this structure, however, requires direct electrophysiological recordings for the *in vivo* characterization of the ion channels that modulate its activity. At present, because of the small size of synaptic terminals in all species, this has been possible in only a very few examples (Llinás et al., 1981; Stanley and Goping, 1991; Forsythe, 1994). Nevertheless, it seems imperative to expand the repertoire of synapses studied, because there is mounting evidence regarding the diversity of components and physiological properties among different synapses (Ullrich et al., 1995; Gardner and Kindler, 1996).

Drosophila has proven to be a fruitful experimental system because of the possibility of using multidisciplinary approaches directed toward a common goal. The K^+ channels were first isolated in this organism (Baumann et al., 1987; Kamb et al., 1987; Tempel et al., 1987), enabling subsequent progress in other species (Jan and Jan, 1992; Pongs, 1992). A similar trend is now developing in the molecular characterization of synapses (for review, see Schwarz, 1994).

Received Dec. 6, 1996; revised Feb. 7, 1997; accepted Feb. 25, 1997.

This research has been funded by grants from the Spanish Dirección General de Investigación Cientifica y Técnia 93-0149 and the European Science Foundation European Neuroscience Programme 16. The critical comments of Drs. J. Lerma, W. Buño, and A. Villarroel are appreciated. Dr. Pal Toth contributed the electron microscopy figure.

Correspondence should be addressed to A. Ferrús, Instituto Cajal (CSIC), Avenida Dr. Arce 37, 28002 Madrid, Spain.

The larval body-wall muscles of *Drosophila* are contacted by three types of synaptic terminals (Atwood et al., 1993; Jia et al., 1993). Type I boutons (up to 5 μm) mediate glutamatergic synaptic transmission (Jan and Jan, 1976; Johansen et al., 1989). They are buried into the muscle and surrounded by subsynaptic reticulum. Type II boutons are small (<2 μm) and express octopamin (Monastirioti et al., 1995). Finally, type III boutons (up to 1.7 × 6 μm) contain large, dense-core vesicles and exhibit insulin-like and proctolin immunoreactivity (Anderson et al., 1988; Gorczyca et al., 1993), suggesting a peptidergic nature.

We have gained access for the first time to *Drosophila* type III boutons, have performed whole-cell and single-channel recordings, and have characterized some of the K^+ channels present in their membrane. Several reasons justify our focus on synaptic K^+ channels. There is a large background of information, thanks to the previous work on the corresponding genes *Sh, Shal, Shab, Shaw, eag, slo*, and *Hk* (Pongs et al., 1988; Butler et al., 1989; Atkinson et al., 1991; Zhong and Wu, 1991; Chouinard et al., 1995). The molecular data demonstrate the possible existence of a very large number of functionally different channels, the biological significance of which remains to be ascertained. The likely heteromeric combination between protein isoforms of this gene family would raise the number of channel assemblies even higher. Work with K^+ channel isoforms demonstrates that this molecular heterogeneity leads to a differential distribution among different tissues, cell types, and membrane compartments (Rudy et al., 1992; Sheng et al., 1992; Veh et al., 1995). In this context, the K^+ channels present in axon terminals are of special interest, because they play a major role in the modulation of neurotransmitter release (Augustine, 1990; Robitaille et al., 1993).

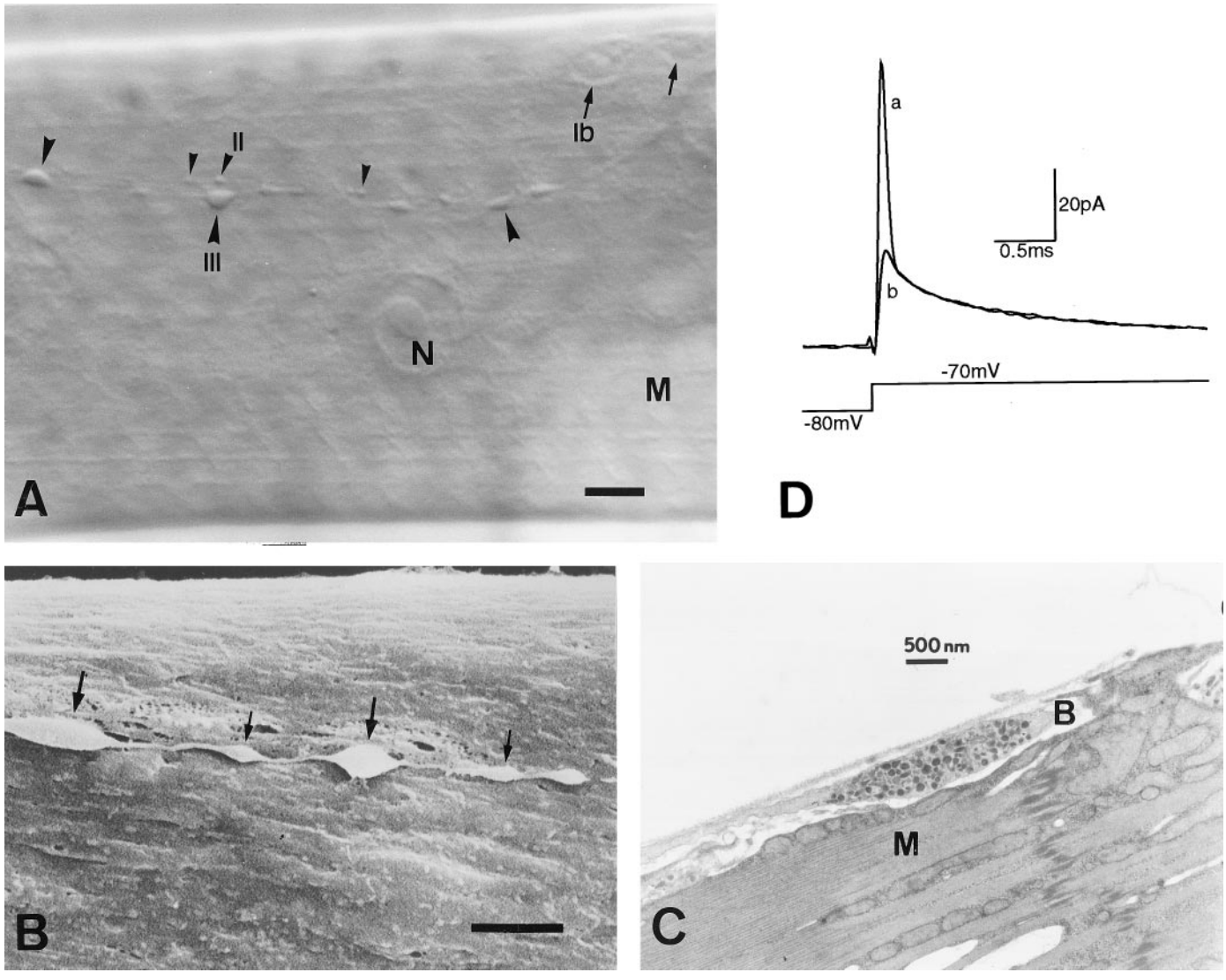

Figure 1. Type III synaptic boutons on *ecd*[1] larval muscle fiber 12. *A*, Nomarski view showing type *Ib* (*arrows*), type *II* (*small arrowheads*), and type *III* (*large arrowheads*) synaptic boutons after collagenase treatment. *B*, Scanning electronmicrograph of type III boutons. Notice the presence of relatively large (*thick arrows*) and small (*thin arrows*) boutons within the same axon string, and also their superficial location and accessible membrane. *C*, Transmission electronmicrograph from a wild type, showing a single type III bouton with a mixed population of dense-core vesicles. Note the elongated shape and the virtual absence of subsynaptic reticulum around the bouton. *N*, Nucleus; *M*, muscle fiber; *B*, synaptic bouton. Scale bar: *A*, 10 μm; *B*, 3 μm. *D*, Synaptic bouton capacitive current before (*a*) and after (*b*) electronic compensation of the first exponential component, in response to a voltage depolarization that elicits passive membrane currents only. The first exponential corresponds to the capacitance of the boutons under the recording pipette. Each trace represents the average of 20 current records.

MATERIALS AND METHODS

Fly stocks. The description of mutants and rearrangements used in this study can be found in Lindsley and Zimm (1992) and Ferrús et al. (1990). The *ecdysone* (*ecd*[1]) allele is a temperature-sensitive recessive lethal (Garner et al., 1977). *ecd*[1] mutant larvae fail to pupate when transferred to 30°C midway through third instar, remaining as larvae for an extended period of time. We have observed that these larvae develop enlarged, type III synaptic boutons (see below). This effect is not detected in type I or type II boutons.

The *Shaker* mutants used to eliminate I_A were Sh^{KS133}, a missense mutation between the S5 and S6 transmembrane-spanning domains and the aneuploid $T(X;Y)B55^{D}$, $B^{S+}/T(X;Y)W32^{P}$, y^+, which removes the entire *Shaker* locus. Other mutants related to the K^+ currents used were *slo*[1], which eliminates the fast Ca^{+2}-dependent K^+ current, and *eag*[1], which reduces several K^+ currents in larval muscles. *ecd*[1] was combined with the other mutations, except for the case of *eag*[1], and homozygous larvae were used for electrophysiological recordings.

Experimental preparation. Cultures of homozygous mutant combinations were routinely kept at 22°C. For experimental recordings, mature *Drosophila* third instar larvae were used 2–4 d after being transferred to 30°C. Larvae were pinned down, dorsal side up, onto a clear Sylgard-coated experimental chamber. The cuticle was cut open along the dorsal midline, and most internal organs were removed, leaving only the CNS connected to the body wall muscle layer. The preparation was then digested for 8–10 min in a solution containing 100 U/ml collagenase (type IA; Sigma, St. Louis, MO), washed thoroughly, and transferred to the microscope for electrophysiological recordings.

Type III boutons are restricted to muscle fiber 12 and occasionally fiber 13. They have a characteristic elongated shape, medium size, and a superficial location. As in wild type, type III boutons in *ecd*[1] appear in a wide range of sizes, even within the same terminal branch (Fig. 1*B*). In the mutant, however, it is common to find boutons of the larger size (~5–6 μm long), which occasionally can be as large as 9 × 3 μm. The boutons were viewed with a 40× water immersion objective under Nomarski optics (Fig. 1*A*), which allows unambiguous identification. All experiments were performed at room temperature.

Electrophysiology. The perforated patch-clamp technique (Horn and Marty, 1988) was used to record whole-terminal and single-channel currents. High-resistance patch pipettes (10–20 MΩ) were pulled from thick-wall borosilicate glass, coated with a layer of Sylgard, and fire-polished. In most experiments, the tip of the pipette was filled with a solution containing (in mM): 130 KCl, 4 $MgCl_2$, 10 HEPES, and 10 EGTA, pH 7.3. The pipette was then back-filled with the same solution to which a saturating concentration of Nystatin (200 μg/ml) was added from a stock solution of 50 mg/ml dissolved in dimethylsulfoxide. The bath solution contained (in mM): 100 NaCl, 5 KCl, 20 $MgCl_2$, 5 HEPES, and 115 sucrose, adjusted to pH 7.3. Gigaseals of up to 30 GΩ were obtained by applying gentle suction after the pipette tip was brought into contact with the membrane of the terminal. To record single-channel currents, perforated vesicles were obtained by switching briefly to current-clamp mode and gently pulling the electrode away from the synaptic bouton. Some experiments were performed in the inside-out configuration using a Nystatin-free pipette solution. In these cases, the pipette tip was exposed briefly to the air and then transferred to a second chamber for perfusion with intracellular solution. Ionic currents were recorded with a patch-clamp amplifier (Axopatch-1D), filtered at 1–2 kHz, digitized, and stored in a computer for further analysis using PClamp software.

Because synaptic boutons are connected to each other through fine, relatively long processes, the charging of the membrane capacitance displays a rapid, single exponential component that represents the charging of the bouton under the recording electrode, followed by a number of smaller, slower exponential components that correspond to the charging of the processes (Jackson, 1992). The bouton capacitance (Fig. 1*D*) and electrode series resistance were determined by adjusting the transient cancellation circuitry of the patch-clamp amplifier (Marty and Neher, 1983) to compensate for the first exponential component of the capacitive charging current elicited by a 10 mV depolarization (from −80 to −70mV), which activates only passive currents. This method was prone to error because of the small magnitude of the capacitance involved. Therefore, we also acquired current records after compensation of the pipette capacitance only and obtained a second estimate of the bouton capacitance and series resistance by fitting several exponential functions to the current transient and integrating the area under the fastest exponential component after subtraction of the leak current.

The fastest component of the charging transient had a capacitance of 1.05 ± 0.13 pF and a decaying time constant of 58.2 ± 3.9 μsec. The associated series resistance was calculated to be 57.4 ± 4.1 MΩ (n = 17), ~3–4 times larger than the pipette tip resistance before a seal was obtained. Without series resistance compensation, the average series resistance introduces a voltage error of ~5 mV for a current magnitude of 100 pA and ~1 mV with 80% compensation. The values of the time constant and series resistance thus calculated determine the speed and quality of the voltage-clamp system for the synaptic bouton immediately under the pipette. The nerve terminals are charged rapidly enough to study the kinetics of K^+ currents described here, provided the ionic channels under study are present in the bouton itself (see Results).

Unless indicated otherwise, macroscopic membrane currents were corrected for leak either on-line, using a P/N 4 protocol, or by subtracting the current produced by a pulse of the same magnitude but opposite polarity. This later method proved to be appropriate, because no active membrane currents were present even at the most extreme hyperpolarized potentials. Single-channel currents were corrected for linear leak and uncompensated capacitive transients by subtracting a template obtained either by fitting smooth functions to current records with no openings or, when possible, by averaging many such records. Pooled data in the text are normally presented as mean ± SEM.

RESULTS

We have assayed several procedures to render *Drosophila* terminals amenable to electrophysiological recordings. These included the use of mutations, such as *gigas*, which yield very large boutons (up to 13 μm) (Canal et al., 1994), *giant*, and *lethal(1) disk large* (Woods and Bryant, 1991), as well as pharmacological treatments promoting cell fusion or polyploidy in primary cultures. In our hands, only the mutant *ecd* proved to be a reliable tool to gain access to larval type III peptidergic boutons.

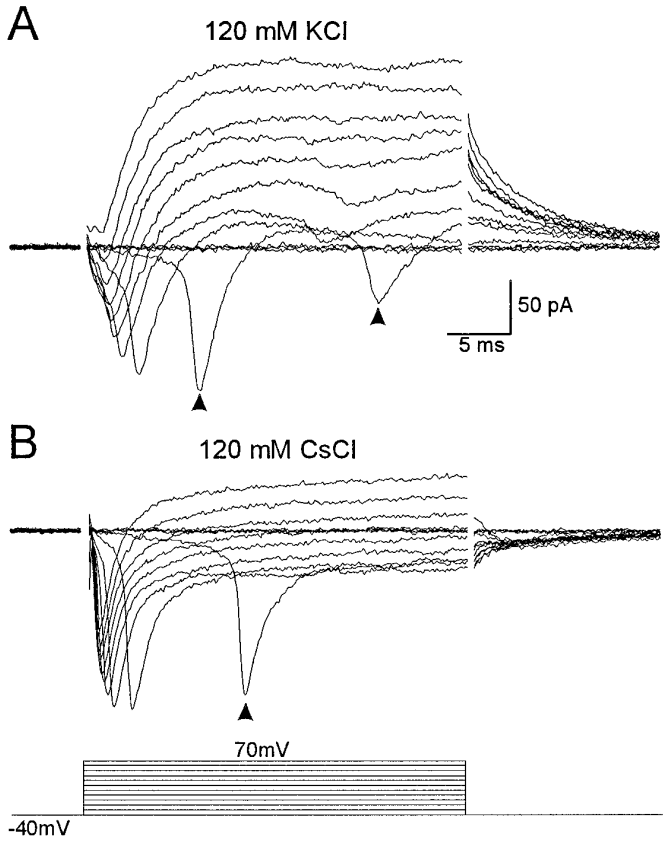

Figure 2. Whole-terminal ionic currents recorded with the nystatin perforated-patch technique. The membrane was depolarized between −40 and 70 mV in 10 mV steps. In *A*, the patch pipette contained standard recording solution (see Materials and Methods). The macroscopic current reveals an inward component attributable to sodium influx (TTX sensitive), followed by a sustained outward component. Notice that the inward Na^+ current is not well controlled under voltage clamp (*arrowheads*), suggesting that it may be generated outside the synaptic bouton. In *B*, the replacement in the patch pipette of K^+ ions with Cs^+ causes a large reduction of the outward component without affecting the Na^+ current, indicating that the outward current is carried mostly by K^+ ions.

Macroscopic currents

A total of 105 type III synaptic boutons innervating muscle fiber F12 were recorded in these experiments. The mean input resistance of synaptic boutons was 8.85 ± 1.06 GΩ (n = 29), and the mean bouton capacitance was 0.98 ± 0.07 pF (n = 21). These boutons displayed various voltage-dependent ionic currents after membrane depolarization. The macroscopic current profile in response to 30-msec-long, increasing voltage steps from a holding potential of −40 mV is shown in Figure 2*A*. In a nominally Ca^{+2}-free extracellular solution, the total macroscopic current consists of an initial, rapidly inactivating inward component that is followed by a delayed, sustained outward current. The inward current is carried by Na^+ ions, because it is completely blocked by including 1 μM tetrodotoxin (TTX) in the extracellular bath (Fig. 3*A*) and by replacement of extracellular Na^+ with a cation, *N*-methyl-glucamine, which does not permeate through Na^+ channels (n = 4; data not shown). In those experiments performed in the absence of TTX, we typically observed repetitive inward currents superimposed on the sustained outward component (*arrowheads*, Fig. 2*A,B*), suggesting that action potentials did indeed arise from poorly space-clamped areas of the membrane,

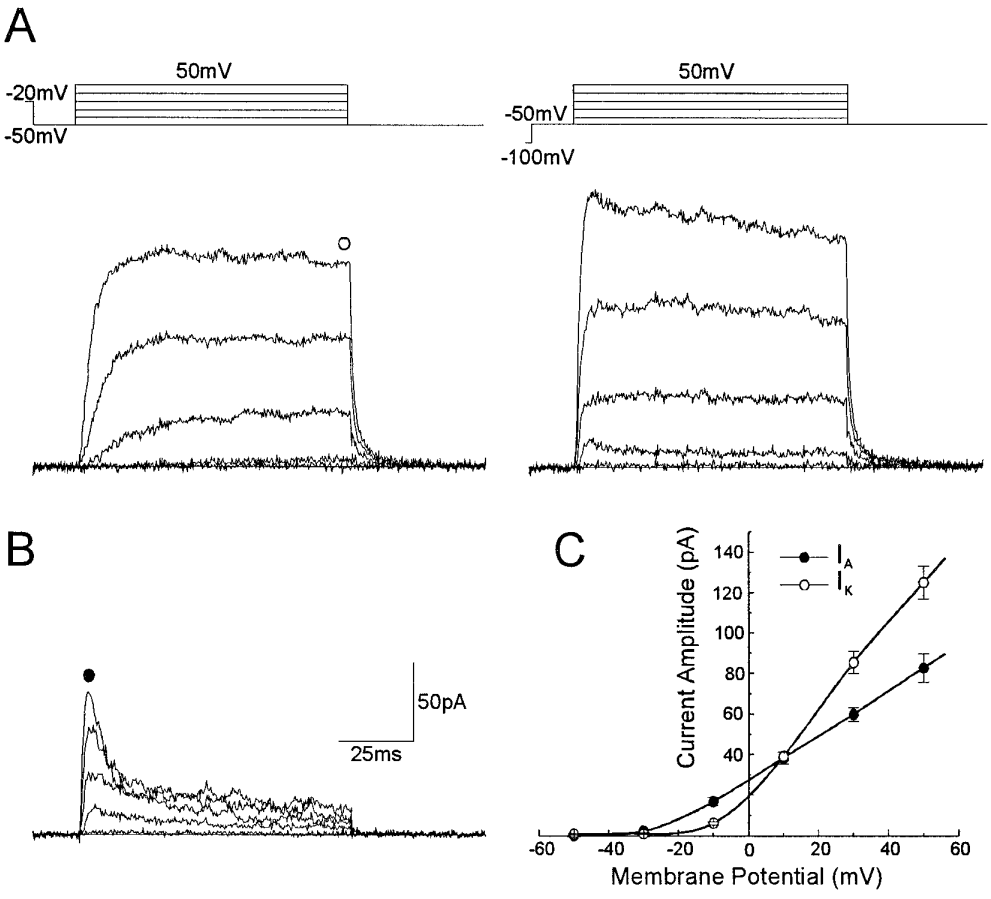

Figure 3. Separation of K^+ current components. The bath solution was nominally Ca^{2+}-free and contained 1 μM TTX to block Na^+ currents. *A*, Membrane currents in response to depolarizing pulses from a holding potential of −50 mV when they are preceded by a 500 msec conditioning to either −20 mV (*left traces*) or −100 mV (*right traces*). The prepulse to −100 mV reveals a transient component at the beginning of the depolarizing pulse that has been isolated in *B* by subtracting both families of traces. *C*, Graphic representation of the peak transient current (*solid circles*; n = 8) and the sustained current measured at the end of the depolarizing pulse (*open circles*; n = 16) plotted against the membrane potential.

outside the synaptic terminal proper. This was supported by two additional observations: (1) the inward current was not present in isolated boutons that had been "pulled out" of the terminal branch, and (2) Na^+ channels were conspicuously absent in our single-channel recordings. In fact, sodium channels may be present in the connecting processes between synaptic boutons. Of seven detached boutons recorded, only one, actually a string of four connected boutons, displayed a remnant inward current. The inward Na^+ current was not studied any further.

The outward current was assumed to be carried by K^+ ions on the basis of the following criteria: (1) the substitution of K^+ with Cs^+ resulted in a large, time-dependent reduction of the outward current (Fig. 2*B*; n = 4); (2) the outward current was not significantly affected by the replacement of chloride with methanesulfonate ions in the extracellular solution (not shown; n = 3); (3) this current was inhibited by potassium channel blockers such as 3,4-diaminopyridine and quinidine (see below); and (4) the kinetics and voltage-dependence of the macroscopic currents are in accordance with the properties of the single K^+ channels described below.

Separation of K^+ currents

To isolate K^+ currents from other ionic currents, experiments were carried out in a nominally Ca^{2+}-free extracellular solution with the addition of 1 μM TTX. Under these conditions, the macroscopic outward current of *Drosophila* synaptic boutons contains at least two kinetically distinct components. The left panel in Figure 3*A* represents the family of currents recorded in response to progressively larger, 90-msec-long voltage steps when these are preceded by a 500 msec conditioning pulse at −20 mV. Membrane depolarization above −20 mV elicits an outward current that reaches a plateau and does not inactivate for the duration of the pulse. Application of a conditioning pulse to −100 mV, however, reveals the presence of a second, rapidly inactivating component at the beginning of the depolarization (Fig. 3*A*, *right*). This second component can be isolated by subtracting the family of currents produced after the conditioning pulse to −20 mV from that obtained after a conditioning pulse to −100 mV (Fig. 3*B*). The transient component thus obtained reveals a rapidly activating current that reaches a peak and almost completely inactivates before the end of the test pulse.

Figure 3*C* shows the *I/V* relationship of the outward currents both at the peak of the transient component (*solid circles*) and at the end of the depolarizing pulse (*open circles*). The *I/V* plot reflects the difference in the activation threshold of both components. The transient current begins to activate at lower voltages, and its amplitude was typically approximately two-thirds of the delayed current (at 50 mV). The properties of the transient K^+ current (i.e., its relative low voltage activation, fast inactivation during membrane depolarization, and voltage-dependent steady-state inactivation; see next section) are similar to those of the transient K^+ current (I_A) originally described by Connor and Stevens (1971b) in molluscan neurons and also present in various preparations, including *Drosophila* muscle fibers (Wu and Haugland, 1985) and neurons (Byerly and Leung, 1988; Solc and Aldrich, 1988; Baker and Salkoff, 1990). On the other hand, the delayed K^+ current resembles I_K as described in molluscan somata (Connor and Stevens, 1971a), *Drosophila* adult and larval muscle (Salkoff and Wyman, 1981; Wu and Haugland, 1985), and

embryonic and larval neurons (Solc and Aldrich, 1988; Tsunoda and Salkoff, 1995b). In this report the transient and delayed K^+ currents will be referred to as I_A and I_K, respectively, notwithstanding that these terms refer to a general type rather than to a single unique current (see Discussion).

The boutons occasionally broke free ($n = 7$) from the arborization when the recording pipette was carefully pulled away from the membrane of the terminal. Membrane resealing at both ends of the bouton, however, allowed stable recordings to be made. The K^+ current components I_A and I_K described above (but not I_{Na}) were still present, although somewhat reduced, in these isolated terminals (not shown), indicating that a large fraction of the K^+ channels underlying both currents are located within the boutons themselves. Moreover, the mean current density at 30 mV for the peak of I_A and I_K steady state were 61 and 87 $\mu A/\mu F$, respectively, i.e., seven to eight times higher than those of I_A and I_K in muscle fibers (Wu and Haugland, 1985).

Kinetics and voltage dependency of I_A

Significant activation of I_A can be detected at membrane potentials above −40 mV. The amplitude of the peak current increases and the time to peak decreases as the membrane depolarizes further. The inactivation profile of I_A was somewhat variable; in some experiments, after an initial rapid current decay, a small steady-state component remained for the entire duration of the depolarization (Fig. 3*B*). The initial phase of the decay could be best-fitted by a single exponential function with a time constant of 6.4 ± 1.05 msec ($n = 8$) at 50 mV and was not strongly voltage dependent, although it became slightly faster with increasing depolarization.

It is clear from Figure 3*A* that the transient K^+ current exhibits voltage-dependent steady-state inactivation. To analyze this property we acquired current traces in response to a constant test pulse to 50 mV after 1-sec-long prepulses at various holding potentials (between −120 mV and −10 mV). The current peak was then normalized to the largest current, produced from a holding potential of −120 mV, and represented as a function of the prepulse potential. As the prepulse potential becomes more hyperpolarized, the transient outward current increases in amplitude (*inset*, Fig. 4*A*). The average data points from seven similar experiments are depicted in Figure 4*A*. The solid line results from fitting to the data points a single Boltzmann function of the form:

$$\frac{I}{I_{Max}} = \frac{1}{1 + e^{(V - V_h)/k}},$$

with a midpoint for steady-state inactivation (V_h) of −62 mV, and a slope factor (k) of 13 mV. The time course of recovery from inactivation was measured using a two-pulse voltage protocol. From a holding potential of −100 mV, a step to a membrane potential of 50 mV was applied to activate the outward current, adjusting the duration of the pulse to completely inactivate the transient component. A second similar pulse was then delivered after returning to the holding potential for a variable length of time. An increase in the interval between pulses elicited an outward current of progressively larger peak amplitude, indicating a recovery from inactivation (Fig. 4*B*) that was typically completed within 1 sec ($n = 3$).

Delayed K^+ current, I_K

The first detectable I_K current was observed at potentials greater than −20 mV, which is somewhat higher than the activation threshold for I_A (Fig. 3*C*). As the voltage command becomes more depolarized, the onset of this current is more rapid and its size increases. Figure 5*A* displays some of the kinetic characteristics of the synaptic I_K. Current traces in response to 60-msec-long depolarizing pulses to various membrane potentials were acquired after a 500 msec conditioning pulse to −20 mV. Under these conditions, the I_A was completely inactivated, allowing the isolation of the I_K without contamination from the transient current. I_K activates more slowly than I_A, following a sigmoid time course that is more apparent at low voltages (Fig. 5*A*, *left traces*). In general, the activation time course was well-fitted by an exponential function raised to the second power (superimposed on the data traces in Fig. 5*A*), suggesting that the channels underlying I_K must proceed through at least two closed states before they open. Furthermore, the corresponding tail currents that developed when the membrane was repolarized to −50 mV were well-fitted

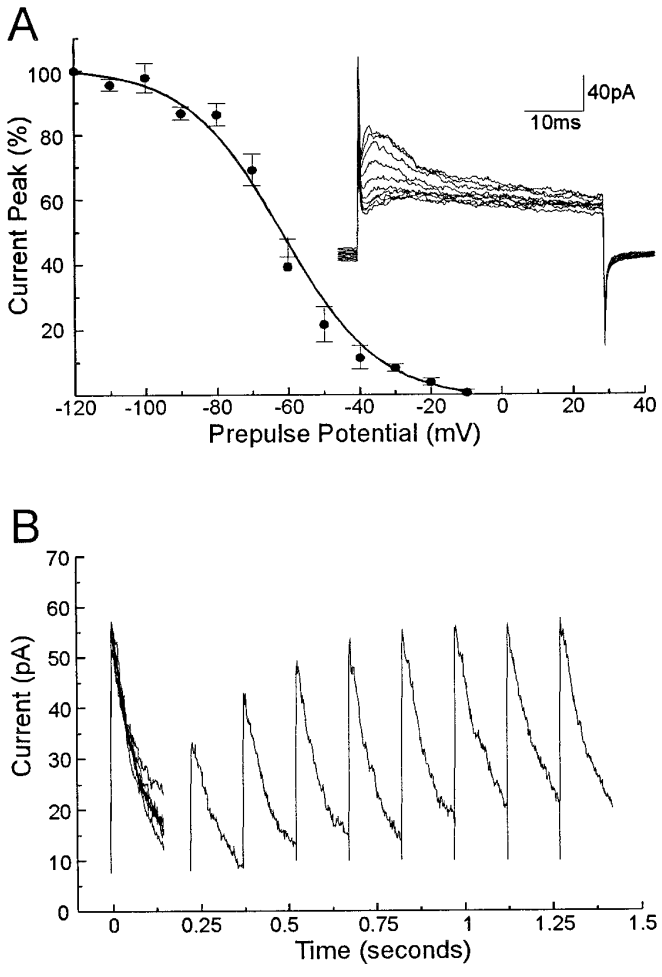

Figure 4. Kinetics and voltage dependence of I_A. *A*, Steady-state inactivation curve. The *inset* represents a series of current traces from an isolated bouton, produced by a test potential to 50 mV after prepulses to a range of membrane potentials between −120 and −10 mV (no leak subtraction was applied). The graph includes pooled data from seven different boutons. Peak amplitudes of I_A were normalized and plotted as a function of the prepulse potential, and the data were fitted with a Boltzmann function with half-inactivation of 62 mV and a slope factor of 13 mV. *B*, Time course of recovery from inactivation. Complete inactivation of I_A was produced by a test command to 50 mV from a holding potential of −100 mV. Recovery from inactivation was tested by returning the membrane potential to −100 mV for a progressively longer time before a second test pulse was applied.

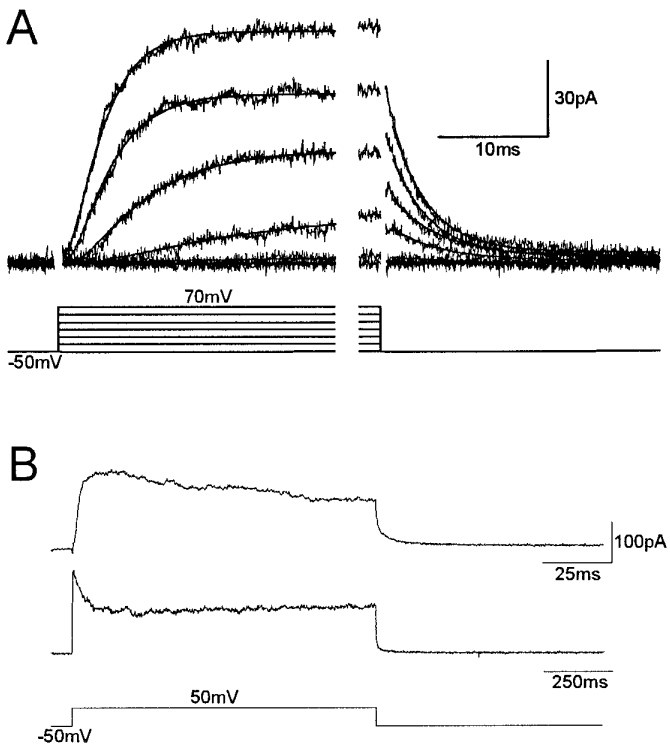

Figure 5. Activation and inactivation of I_K. In *A*, the activation of I_K (after inactivation of I_A by a prepulse to −20 mV) follows a sigmoid kinetics that is best-fitted by a double-power exponential function (superimposed in the *left traces*). The membrane was depolarized from a holding potential of −50 mV in 20 mV steps. *Traces* on the *right* represent tail currents from the same bouton after membrane repolarization after a 60 msec pulse, and they were well-fitted by a single exponential function with a time constant of 5–6 msec. *B*, I_K slow inactivation during prolonged depolarization. Two current traces at two different time scales are displayed to illustrate the inactivating nature of I_K. The delayed current recorded in response to long depolarizing pulses always exhibits a similar profile with a slowly inactivating and a noninactivating component.

by a single exponential function with a time constant of 5–6 msec (Fig. 5*A*, *right traces*). That only a single exponential function is required to fit the tail currents time course suggests that a single kinetic K^+ component contributes to the sustained current.

The time course of the delayed K^+ current when the membrane was depolarized for greater lengths of time is depicted in Figure 5*B*, revealing that I_K undergoes a slow inactivation process that was not apparent with short pulses. The figure shows that after an initial slow decay the macroscopic current reached a noninactivating plateau phase lasting for the entire duration of the depolarization (up to 1.5 sec). The macroscopic current represented in Figure 5*B* exhibited a relatively fast and pronounced inactivation and was specifically selected to illustrate the inactivating nature of I_K; however, all boutons recorded ($n = 8$) had a delayed K^+ current that inactivated to some extent within this time scale.

The K^+ currents were characterized further by examining their sensitivity to a number of classic K^+ channel blockers, including 3,4-DAP, tetraethylammonium (TEA), and quinidine. In general, the effects of all the channel blockers were not specific to any particular current component. Quinidine seems to be the most selective, and when applied to the extracellular solution at 100 μM it caused a 75% reduction in I_K ($V_C = 40$ mV; $n = 3$) and a slight (17%) reduction in I_A. Conversely, 3,4-DAP (30 μM), which blocks I_A from *Drosophila* muscle (Gho and Mallart, 1986), had almost no effect on synaptic I_K (10%) and blocked only ~49% of synaptic I_A ($n = 3$). The quinidine effect is consistent with that shown in larval muscles (Singh and Wu, 1989), whereas 3,4-DAP shows less effect on synaptic I_A. Finally, in the case in which TEA (10 mM) was added to the bath solution, I_K and I_A were reduced to 31% and 47%, respectively, of their control values. Because these standard K^+ channel blockers did not yield specific effects with respect to either I_A or I_K, no further attempt at pharmacological characterization was pursued.

Genetic analysis of K^+ currents from synaptic boutons

Four different K^+ current components, either voltage- or Ca^{+2}-activated, are present in *Drosophila* larval muscle fibers (Wu and Haugland, 1985; Gho and Mallart, 1986; Singh and Wu, 1989). The voltage-activated K^+ currents include a rapidly inactivating current (I_A) and a slow delayed-rectifier current (I_K). The Ca^{+2}-activated currents can also be classed according to their inactivation rate with a fast (I_{CF}) and a slow (I_{CS}) component (Salkoff, 1983; Gho and Mallart, 1986; Singh and Wu, 1989).

The muscular and some neuronal I_A are encoded by the *Shaker* gene (Salkoff and Wyman, 1981; Wu and Haugland, 1985; Baker and Salkoff, 1990). The properties of I_A from muscle and neuron somata are somewhat different from those of the I_A present in the synaptic boutons. In particular, the voltage-sensitivity of muscular I_A steady-state inactivation is displaced toward more positive potentials. Differential splicing of the *Shaker* locus produces a remarkable diversity of gene products (Kamb et al., 1988; Pongs et al., 1988), which might result in many types of I_A with different properties, depending on the channel subunit composition. Alternatively, synaptic I_A might be encoded by a different gene. We tested these possibilities by examining synaptic K^+ currents in *Shaker* mutants that eliminate I_A in larval and adult muscle. Figure 6*A* shows a family of K^+ currents activated by depolarizing pulses both in ecd^1 and $ecd^1\ Sh^{KS133}$ muscle fibers. The transient current that becomes active (Fig. 6, *arrow*) at the beginning of the pulse in ecd^1 muscle fibers is completely absent in the *Shaker* mutant. By contrast (Fig. 6*B*), synaptic boutons from Sh^{KS133} larvae exhibit an I_A current entirely analogous to, in terms of both amplitude (Fig. 6*C*) and kinetics ($\tau_i = 7.5 \pm 0.6$ msec; $n = 6$), its wild-type counterpart. More importantly, a physical deletion of the entire gene obtained in the aneuploid $T(X;Y)B55^D$, $B^{S+}/T(X;Y)W32^P$, y^+, also results in a normal I_A synaptic current. Thus, it can be concluded that this current is unrelated to *Shaker*.

Slowpoke (*slo*) is a gene that encodes the K^+ channel underlying I_{CF}, and null mutations for the *slo* gene specifically eliminate I_{CF} in muscle and neuron somata (Elkins et al., 1986; Singh and Wu, 1989; Komatsu et al., 1990). It is unlikely that synaptic I_A corresponds to the fast Ca^{+2}-activated K^+ current, because it can be activated in nominally Ca^{+2}-free extracellular solution, although we have not studied its calcium dependence. Consistent with this, normal I_A currents were recorded from synaptic boutons homozygous for the slo^1 mutation ($n = 4$; not shown).

The *ether-à-go-go* (*eag*) gene encodes a polypeptide that shares sequence homology with several K^+ channels (Warmke et al., 1991). When injected into *Xenopus* oocytes, *eag* mRNA induces the expression of a noninactivating voltage-dependent channel that permeates both K^+ and Ca^{+2} ions (Brüggemann et al., 1993). Because *eag* mutations do not eliminate any single K^+ current but do have effects on all known K^+ currents from muscle, it has been suggested that *eag* provides a subunit that is common to several voltage-dependent K^+ channels (Zhong and Wu, 1991, 1993). Only three synaptic boutons from eag^1 larvae were recorded as a

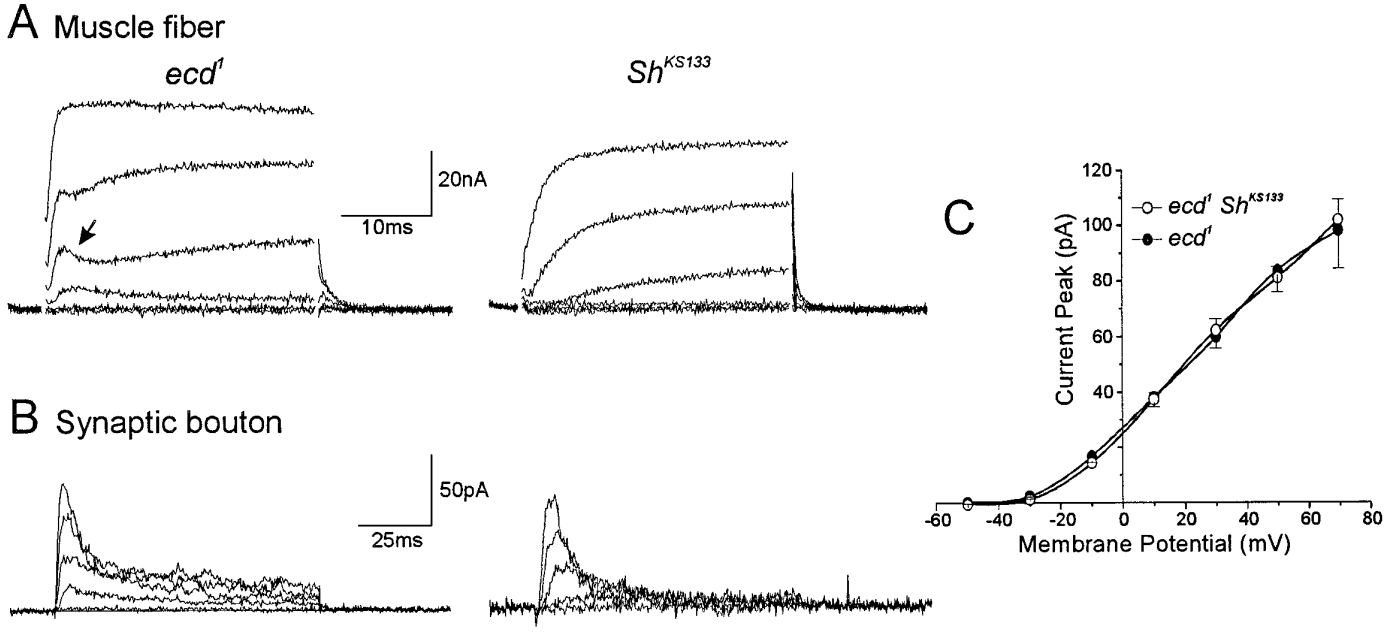

Figure 6. Synaptic I_A is not encoded by *Shaker*. *A*, Macroscopic K^+ currents recorded under two-electrode voltage clamp in body-wall muscle fibers from ecd^1 (*left traces*) and ecd^1 Sh^{KS133} (*right traces*) larvae. Note that the muscular I_A (*arrow*) present in ecd^1 mutants is selectively eliminated by the *Shaker* mutation. *B*, Macroscopic I_A current in synaptic boutons from ecd^1 (*left traces*) and ecd^1 Sh^{KS133} (*right traces*) mutants. Note that unlike the muscle current, synaptic I_A is still present in *Shaker*. *C*, Graphic representation of the peak transient current versus membrane potential for ecd^1 (*solid circles*; $n = 8$) and ecd^1 Sh^{KS133} (*open circles*; $n = 7$) boutons. The voltage protocol was the same as in Figure 3.

result of the difficulty in finding boutons large enough, because *eag* was not combined with ecd^1. Nevertheless, I_A in eag^1 mutants seemed to inactivate four times slower than in control larvae (τ_i = 25.8 ± 5.2 msec; $n = 3$; not shown). These results, albeit preliminary, are consistent with those of Chen et al. (1996) showing that coexpression in oocytes with *eag* increases the inactivation rate of *Shaker* currents, and they seem to indicate that *eag* can also interact functionally with the channels that underlie synaptic I_A, as has been suggested for other K^+ channels (Zhong and Wu, 1991, 1993).

Single potassium channels

At least three different voltage-activated K^+ channels with distinct conductance, kinetics, and voltage-dependent properties are found consistently in the membrane of type III synaptic boutons. Because the extrapolated reversal potential for all three channels is more negative than −50 mV, they are mainly selective for K^+, the only ion with a negative equilibrium potential in our recording conditions. Also, because all the channels can be activated in a nominally Ca^{+2}-free extracellular solution, none of the channels are strictly calcium-dependent. The combination of all three channel types may largely account for the macroscopic current recorded at the level of the whole terminal. In contrast, single sodium channels were never observed in our experimental conditions (100 mM extracellular NaCl). This, together with the observation that the TTX-sensitive inward current is not present in isolated boutons, strongly suggests that type III synaptic boutons do not contain sodium channels. The following description is based on recordings from more than 80 membrane patches, in both perforated vesicle and inside-out patches.

A_2 (*Shal*-like) channels

In perforated vesicles, we have identified a channel type that because of its kinetics and voltage dependence may be responsible for the macroscopic fast transient K^+ current recorded in these boutons. This channel, according to its biophysical properties, seems to correspond to the A_2 channels found in larval CNS neurons (Solc et al., 1987; Solc and Aldrich, 1988) and also to the *Shal* channels as described in embryonic neurons (Tsunoda and Salkoff, 1995a).

In response to a depolarizing pulse (more +30 mV than −30mV) from a hyperpolarized membrane potential (−100 mV), A_2 channels typically display many brief openings (mean open time <1 msec) clustered at the beginning of the depolarization, although the channels may reopen later during the pulse (Fig. 7*A*). Consistent with this, ensemble average currents displayed a sequence of rapid activation followed by rapid inactivation, sometimes with a small steady-state component, which closely resembled the current profile of the macroscopic I_A. Perforated vesicles containing only one A_2 channel were seldom found; rather, several channels were often present in the same membrane patch, suggesting that A_2 channels may be distributed in clusters.

The inactivation rate of ensemble currents from multichannel vesicles presented certain variability. In general they could best be fitted either by a single exponential with a fast time course (τ = 3.9 msec) or by a double exponential function (τ_1 = 3.6 msec, τ_2 = 61.4 msec). In the latter case, single-channel openings with longer open times (*last trace* in the *right panel*, Fig. 8*A*) were relatively frequent. This is consistent with the results of Solc and Aldrich (1988) and Tsunoda and Salkoff (1995a), suggesting that *Shal* channels may exhibit two distinct gating modes with different inactivation rates. The current inactivation rate was little affected by the level of depolarization (not shown), which is also a characteristic of *Shal* versus *Shaker*-coded channels.

To determine the unitary conductance of A_2 channels ($n = 7$), we applied voltage ramp commands from a hyperpolarized membrane potential to obtain channel openings at a wide range of

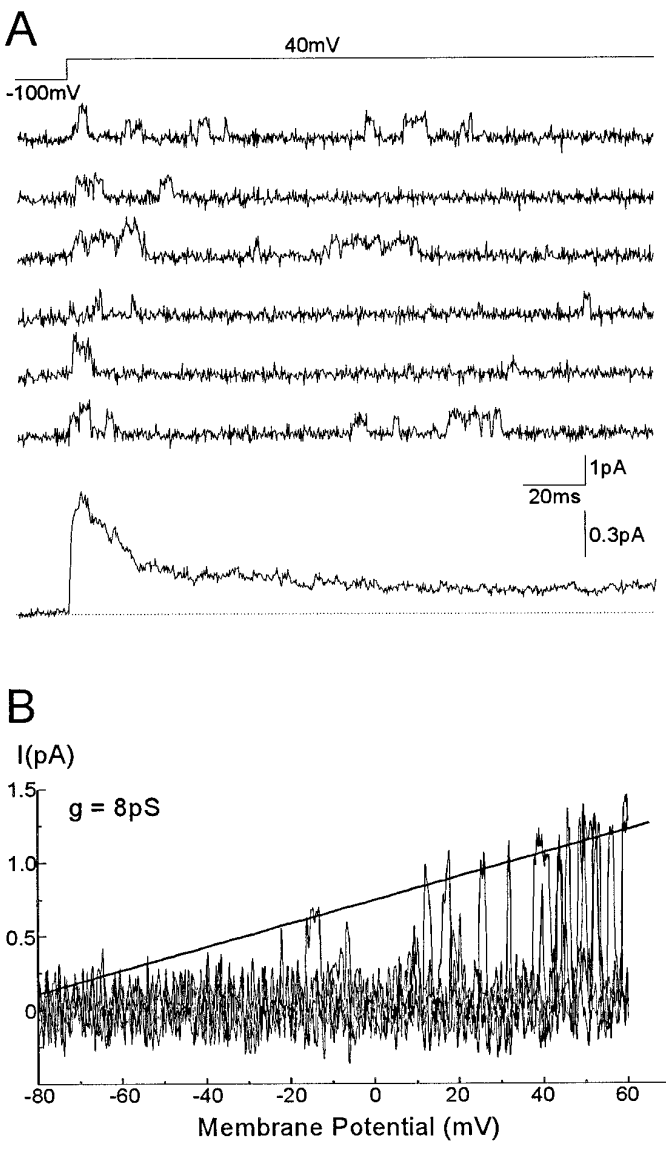

Figure 7. Single-channel currents through A_2 channels. *A*, Representative current records from a perforated vesicle, in response to repetitive voltage steps from −100 to 40 mV. The resulting ensemble average current from 200 similar records is displayed below. *B*, Single-channel current–voltage relationship generated by a ramp voltage command from −100 to 60mV. A line fitted by eye to the opening events yields a unitary slope conductance of 8 pS and a reversal potential at around −80mV.

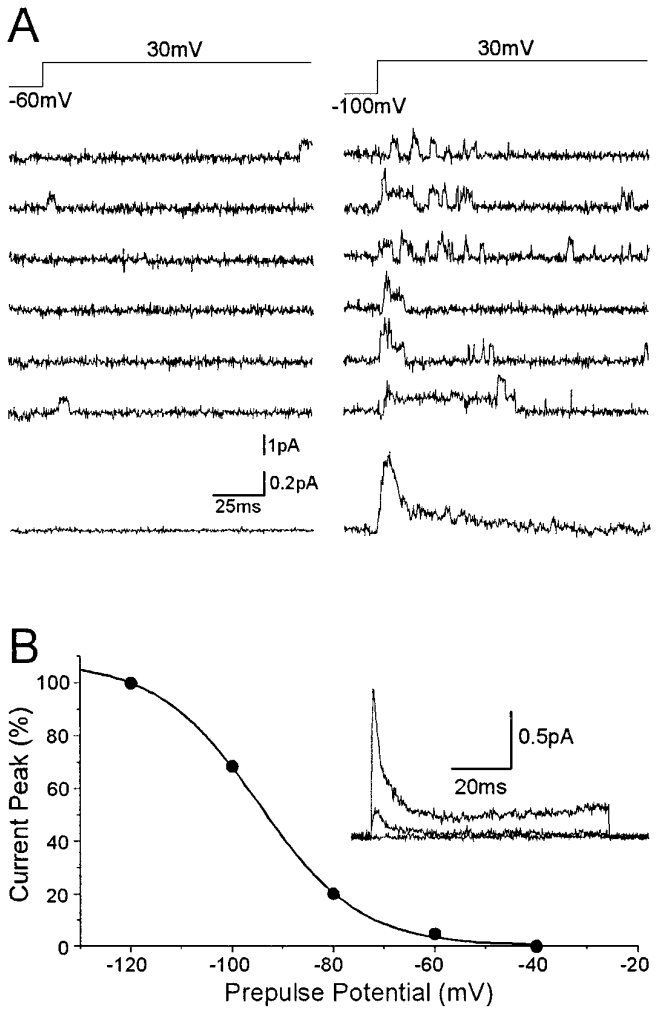

Figure 8. Steady-state inactivation properties of A_2 channels. *A*, Consecutive records of single-channel currents from a patch containing several A_2 channels, in response to voltage steps to 30mV from either −60 (*left*) or −100mV (*right*). Current records from a prepulse to −60 contain few brief channel openings, whereas almost all records from prepulses to −100 mV display multiple single-channel events. *B*, Prepulse inactivation of A_2 channel ensemble average. The *inset* shows a series of ensemble currents generated by a step to 40 mV from −120, −80, and −40 mV. The largest current corresponds to a prepulse to −120mV. The plot represents the normalized ensemble current amplitudes versus the prepulse voltage. The *solid line* represents the best fit to a Boltzmann equation for this particular patch (see text).

membrane potentials. Figure 7*B* displays the unitary current amplitude versus the membrane potential for A_2 channels, when the channel was activated by a voltage ramp command from −100 to 60 mV. A linear fit of the data gives a conductance of 8 pS and a reversal potential around −80 mV. A_2 channels in other patches yielded conductance values ranging from 6 to 8.7 pS.

Like the macroscopic I_A current, A_2 channels also display voltage-dependent steady-state inactivation. Figure 8*A* shows A_2 single-channel openings, from a perforated vesicle containing at least two channels, in response to a depolarizing pulse of 30 mV, when the voltage step is preceded by a 500 msec conditioning pulse of either −60 or −100 mV. From a holding potential of −60 mV, channel openings are rare, whereas current records at −100 mV display frequent multiple channel openings. Figure 8*B* (*insert*) shows ensemble average currents from another patch containing several A_2 channels, recorded at 40 mV, after prepulses to −120, −80, and −40 mV. A representation of the ensemble peak current versus the preconditioning voltage is shown in Figure 8*B*. The solid line corresponds to a Boltzmann equation with a half-inactivation voltage of −94 mV and a slope *k* of 10 mV. In most patches, A_2 channels were inactivated completely with a prepulse to −60 mV. The steady-state inactivation midpoint for A_2 channels was more hyperpolarized than that of the whole-terminal potassium current. A similar and so far unexplained discrepancy between whole-cell and single-channel recordings has been reported previously for *Shal* channels (Tsunoda and Salkoff, 1995a).

K_D (*Shab*-like) channels

Two delayed K^+ current components seemed to be present in type III synaptic boutons. One of them, which we have labeled I_K,

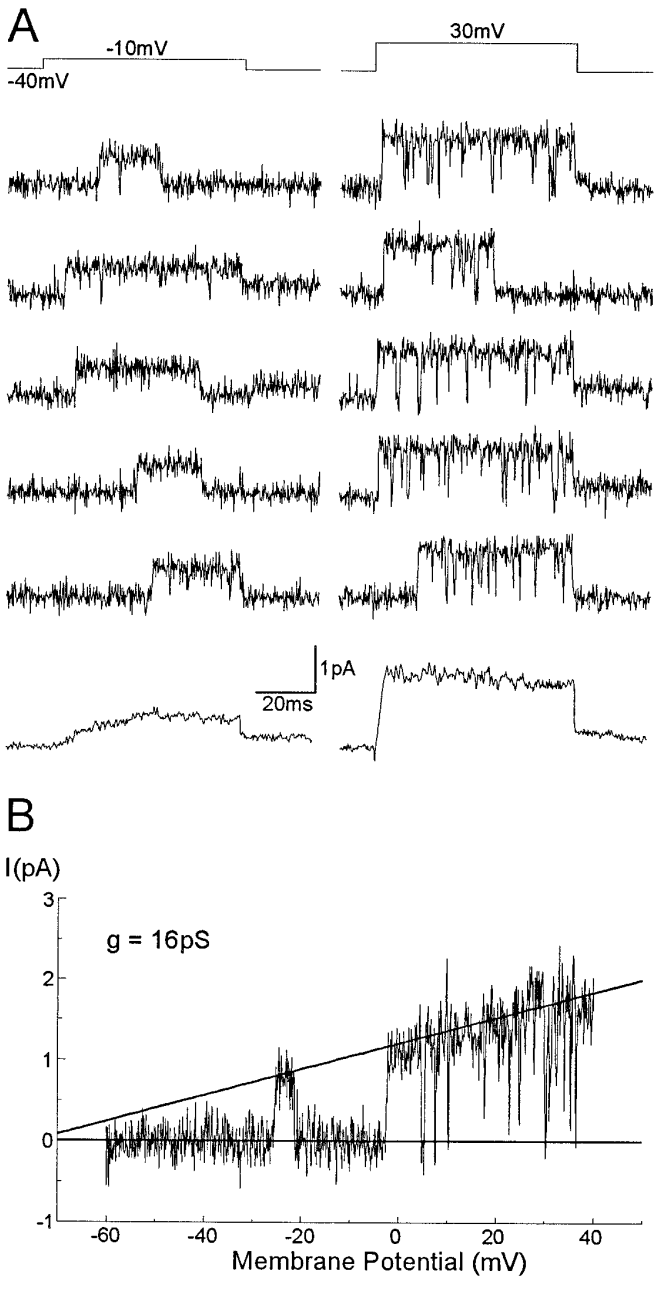

Figure 9. Single K_D channel currents recorded in perforated vesicles. *A*, Single K_D channel and ensemble average currents generated by steps to −10 (*left*) and 30 mV (*right*) from a holding potential of −40 mV. *B*, Single-channel current–voltage relationship generated by a ramp voltage command from −60 to 40mV. A line fitted by eye to the opening events yields a unitary slope conductance of 16 pS and a reversal potential of approximately −70mV.

underwent slow inactivation under prolonged depolarization and during repetitive stimulation. A population of voltage-sensitive channels (K_D channels) previously described in both larval CNS neurons (Solc and Aldrich, 1988) and cultured embryonic myotubes (Zagotta et al., 1988) and possibly encoded by *Shab* (Tsunoda and Salkoff, 1995a,b) may be responsible for this slowly inactivating component of the macroscopic current.

Selected single K_D-channel current records generated by 80-msec-long depolarizing pulses to −10 and 30 mV from a holding potential of −40 are displayed in Figure 9*A*. At membrane potentials of approximately −10 mV and above, K_D channel openings occur after a short delay and are usually long, frequently spanning the whole duration of the depolarization. Long openings are typically interspersed with very brief transitions to the closed state. Increasing the intensity of membrane depolarization reduced the latency to the first opening and increased the flickering of the channel. These channel properties were reflected in the ensemble average current (Fig. 9*A*, *lower traces*), which activates with a slower time course than A_2 channels, its rate of rise increasing with membrane depolarization, and it usually did not inactivate during the 80 msec duration of the pulse. The ensemble current profile of K_D channels resembled the whole-terminal I_K displayed in Figures 3*A* and 5*A*.

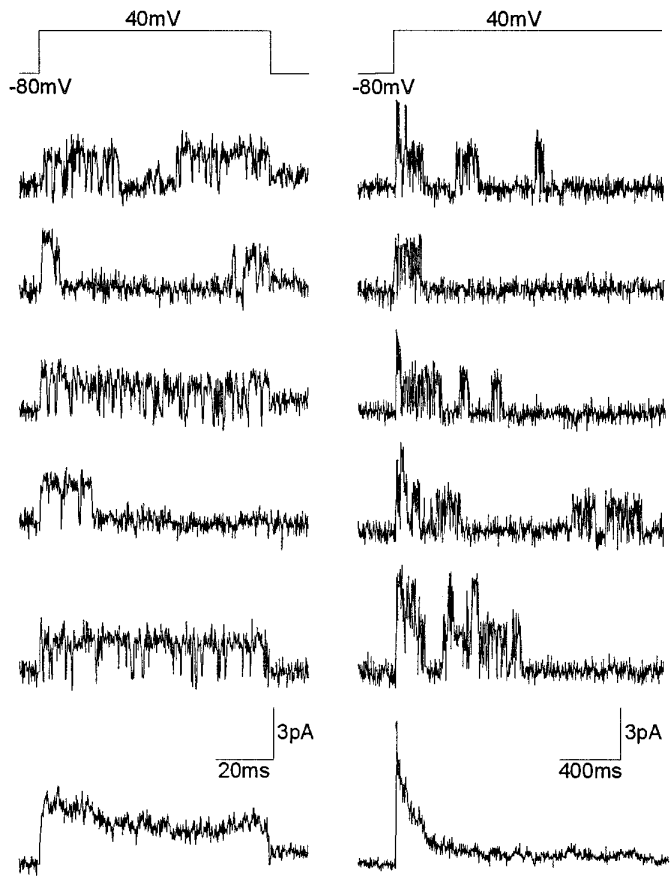

Figure 10. K_D channels inactivate during prolonged depolarization. Single K_D channels activated by short (80 msec) depolarizing pulses and the resulting ensemble average current are displayed in the *series* of *traces* on the *left*. With long depolarizing pulses (1 sec) channel openings tend to cluster at the beginning of the pulse, producing an inactivating ensemble current (*right traces*).

The single-channel current increased linearly with membrane potential. The channel slope conductance ($n = 13$) calculated by applying either voltage ramp commands from −60 to 40 mV (Fig. 9*B*) or serial voltage steps to a range of membrane potentials, fell between 13 and 16 pS, with a reversal potential around −70 mV.

During repetitive depolarizing pulses, K_D channel openings very often clustered in time, with repetitive openings usually followed by periods of silence. This suggests the presence of a slow inactivating process. With long depolarizing voltage pulses, K_D channels readily inactivated. Figure 10 shows current recordings from a perforated vesicle containing at least two K_D channels. With short pulses (80 msec), channel openings lasting for the

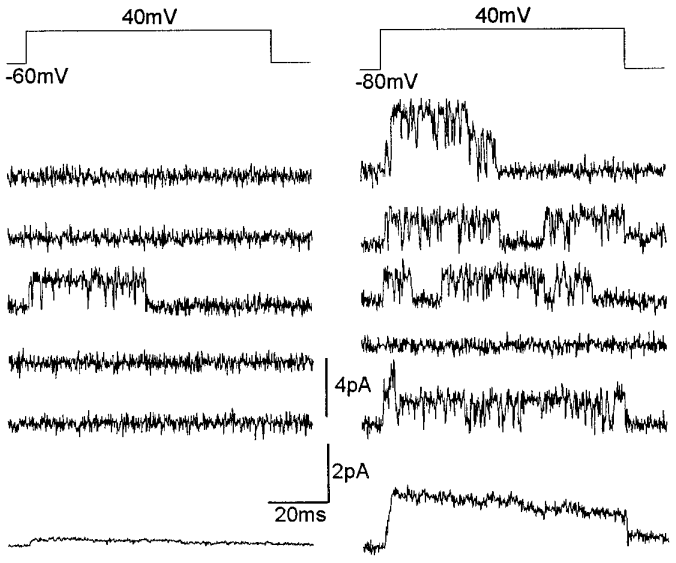

Figure 11. Prepulse inactivation of K_D channels. Single K_D channel openings in response to a depolarizing pulse of 40 mV from a holding potential of either −60 mV (*left traces*) or −80 mV (*right traces*). This patch contained two K_D channels. At −60 mV channel openings were rare; changing the holding potential to −80 mV had an effect on the opening probability that resulted in a considerably larger ensemble current (see text).

whole depolarization were frequent, and the ensemble average current showed little inactivation (Fig. 10, *left*). When the same patch was depolarized with longer pulses, however, channel openings tended to cluster at the beginning of the depolarization, and the average current completely inactivated within 500 msec (Fig. 10, *right*). Within this time scale, the channels displayed a bursting behavior; channel openings typically clustered in long bursts with brief transitions to the closed state, separated in turn by long duration closings.

The slow inactivation of K_D channels suggests that they may undergo voltage-dependent steady-state inactivation. Although we did not systematically study this channel property for the whole range of membrane potentials, the prepulse inactivation of K_D channels seemed to be quite variable, but never as negative as that of A_2 channels. The channel depicted in Figure 9*A* displayed a similar open probability when activated with a 500-msec-long prepulse potential to either −80 mV (not shown) or −40 mV. Figure 11, however, shows another vesicle containing two K_D channels with a more negative prepulse inactivation. Thus, in this patch, changing the conditioning prepulse from −60 mV to −80 mV greatly increased the open probability of the channels and consequently the magnitude of the ensemble average current. This type of behavior has already been reported for K_D channels from CNS neuronal somata (Solc and Aldrich, 1988, their Fig. 13).

K_L (*Shaw*-like) channels

The second component of the whole-terminal delayed current was a truly sustained current that showed no inactivation with pulses as long as 1.5 sec (Fig. 5*B*). Figure 12 depicts single-channel recordings from a third type of channel (K_L) that may contribute to this component of the delayed K^+ current. K_L channel openings with a complex gating kinetics occurred immediately after membrane depolarization, normally spanning the entire duration of the voltage command. This single-channel behavior produced ensemble average currents that activated very rapidly and did not

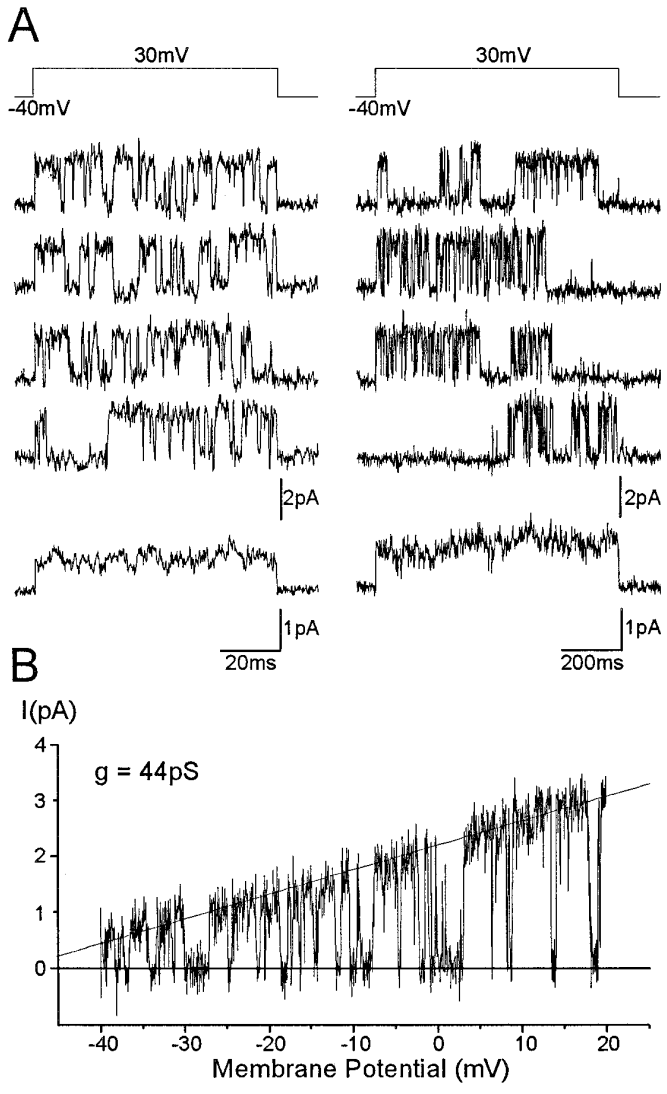

Figure 12. Single K_L channels in perforated vesicles. *A*, Single-channel recordings in response to a membrane voltage step to 30 mV of either 80 msec (*left traces*) or 800 msec (*right traces*) duration, showing the noninactivating nature of the current carried by K_L channels. *B*, Single-channel *I/V* relationship of K_L channels obtained by applying voltage ramp commands from −40 to 20 mV. A linear fit to the data for this particular patch gave a slope conductance of 44 pS.

inactivate with pulses long enough to cause complete inactivation of K_D channels (Fig. 12*A*, *right traces*; compare with Fig. 10).

When the membrane was depolarized with voltage ramp commands, K_L channel openings could be detected at very low potentials (−50 mV). This is in contrast to K_D channels, which under the same stimulation protocol tended to open at more depolarized potentials; openings below −20 mV were infrequent.

The single-channel *I/V* relationship for a patch containing one K_L channel, obtained by applying ramp commands between −40 and 20 mV, is displayed in Figure 12*B*. A linear fit by eye to the data gave a slope conductance of 44 pS. The unitary conductance of K_L channels in other patches was in the range of 44 to 54 pS ($n = 11$). K_L channels did not seem to undergo voltage-dependent steady-state inactivation, and they readily opened when activated from a holding potential of −40 mV.

The major features of the macroscopic currents and single channels are summarized in Table 1.

Table 1. Functional properties of type III bouton macroscopic and single-channel K^+ currents

Macroscopic current	Maximum current amplitude (50 mV)	Activation threshold (mV)	τ for inactivation	S–S inactivation $V_{½}$ (mV)
I_A	82 pA[a]	−30 to −20	6.4 msec	−62
I_K	125 pA	−20 to −10	Slow inactivation	None
Channel type	g (pS)	Activation threshold	τ for inactivation	S–S inactivation $V_{½}$ (mV)
A_2	6–9	~−30 mV	τ = 3.9 msec τ_1= 3.6, τ_2 = 61.4	−94
K_D	13–16	~−20 mV	>150 msec	Highly variable
K_L	44–54	~−50 mV	Noninactivating	None

[a]This value is somewhat underestimated, because the subtraction protocol to isolate I_A required the membrane to be held at −50 mV for a brief period before the depolarizing pulse, which would result in partial inactivation of the current.

DISCUSSION

In this report we describe the voltage-dependent K^+ currents and channels likely to mediate them, present in type III synaptic boutons of *Drosophila*. These ion currents are referred to as I_A and I_K, even though these terms most likely include several hundred current types with distinct biophysical and molecular peculiarities.

In *Drosophila*, the main α-subunits that form K^+ channels are encoded by the four genes *Sh, Shal, Shab*, and *Shaw* (Pongs et al., 1988; Butler et al., 1989; Wei et al., 1990), some of which yield multiple isoforms by differential splicing (Isacoff et al., 1990), whereas associated β-subunits are encoded by *Hyperkinetics* (Chouinard et al., 1995; Wang and Wu, 1996). In addition to these genes, *eag* encodes a protein with sequence homology to K^+ channels (Warmke et al., 1991), which has been proposed as a common subunit of several K^+ channels (Zhong and Wu, 1991, 1993; Chen et al., 1996). At present, this molecular diversity surpasses the described repertoire of voltage-dependent K^+ currents, hence the need to carry out *in situ* studies.

In type III boutons, the macroscopic K^+ current shows three components: (1) a rapidly inactivating I_A, (2) a slowly inactivating I_K, and (3) a noninactivating delayed component. These K^+ currents are not strictly Ca^{+2}-dependent, because they can be activated in a nominally Ca^{2+}-free extracellular solution. Most probably, synaptic boutons also contain one or more Ca^{2+}-dependent K^+ currents, as suggested by preliminary experiments showing an increase in the total outward current after perfusion of the bouton with an extracellular solution containing 1 mM Ca^{2+} (our unpublished observations).

At the single-channel level, three different channel types, with properties that resemble the components of the macroscopic current, are present in a high proportion of the patches. This allows us to propose a correlation between currents and channels. Thus, A_2 channels exhibit hyperpolarized steady-state inactivation and produce ensemble currents that inactivate with a time course similar to I_A, K_D channels inactivate with a much slower time course characteristic of I_K, and K_L channels produce noninactivating ensemble average currents.

The genetic analysis has enabled us to discriminate between the various gene products that yield functional K^+ channels in heterologous expression systems. The mutant phenotypes of *Shaker* demonstrate that it encodes the rapidly inactivating K^+ current in muscles (Salkoff and Wyman, 1981; Wu and Haugland, 1985). In dissociated embryonic nervous systems, however, only a fraction of the neurons contain a *Shaker*-encoded current (Baker and Salkoff, 1990), and most of the neuronal transient K^+ current is attributable to *Shal* (Tsunoda and Salkoff, 1995a). Nevertheless, there is indirect evidence that *Shaker* channels are present in type I motor terminals (Mallart et al., 1991; Gho and Ganetzky, 1992). We have benefited from the genetic analysis to show conclusively that type III boutons, at least, do not express *Shaker* I_A currents, nor do these α-subunits contribute to any of the other K^+ currents studied in these terminals. It is likely that I_A in type III synaptic terminals is encoded by *Shal*, although we cannot provide a direct demonstration because the available deletions of this gene are lethal at the embryo stage (Tsunoda and Salkoff, 1995a). Like the *Shal* current, the steady-state inactivation midpoint of synaptic I_A is hyperpolarized, and its inactivation rate is not strongly affected by voltage. Also, A_2 channels exhibit biophysical properties similar to those of *Shal* channels, including a small unitary conductance and a very hyperpolarized voltage-dependent steady-state inactivation.

In neuronal somata, *Shal* channels exhibit either a fast or a slow gating mode, the relative proportion of channels in each mode giving rise to macroscopic currents with a wide range of inactivation rates (Solc and Aldrich, 1988; Tsunoda and Salkoff, 1995a). In type III terminals, the inactivation rate of synaptic I_A was fast and relatively constant in between boutons. Most A_2 channels displayed very brief openings, although A_2 channels with longer open times were also seen occasionally. If A_2 channels are in fact encoded by *Shal*, it would seem that in synaptic terminals most channels are in the fast gating mode. The limited data obtained on *eag* mutants represent *in situ* evidence that *eag* might interact with *Shal*, in a manner similar to that proposed with respect to *Shaker* (Chen et al., 1996), i.e., an increase in the inactivation rate of *Shal* currents. We have not performed single A_2-channel recordings from *eag* mutants, but a possibility currently considered is that the fast gating mode of *Shal* represents a multimeric channel that incorporates *eag* subunits, whereas the slow mode lacks them.

Among the K^+ channels found in this study, K_D channels are the only ones that produce a slowly inactivating current profile. It is likely therefore that they are responsible for the slowly inactivating component of the delayed current. Nevertheless, some differences exist between the macroscopic and the single-channel currents. In some but not all vesicles, the open probability of K_D channels was increased by prepulses to hyperpolarized membrane potentials, indicating that they may undergo steady-state inactivation. Single K_D channels from larval neurons displayed a similar

variability in the voltage dependence of steady-state inactivation (Solc and Aldrich, 1988). We could not find evidence, however, of any steady-state inactivation for the macroscopic current. In those experiments designed to test the inactivation properties of I_A, hyperpolarized prepulses occasionally caused a slight increase in the current at the end of the test pulse, but with a voltage-dependence similar to that of the peak current. We therefore attributed the current difference to a small steady-state component of I_A (which we could also observe at the single-channel level) rather than to an effect of the prepulse potential on I_K.

Most of the delayed K^+ current in embryonic muscle fibers and neurons is attributable to *Shab* (Tsunoda and Salkoff, 1995b). *Shab* channels have a unitary conductance of 11 pS, exhibit bursting behavior, and produce a slowly inactivating ensemble average current. These properties are similar to those of K_D channels from larval CNS neurons (Solc and Aldrich, 1988) and embryonic myotubes (Zagotta et al., 1988), and they also match those of K_D channels from synaptic boutons, suggesting that they may be encoded by the *Shab* gene as well. In this respect, I_K was not affected by *Shaker* null mutations (not shown), which rules out the possibility of it being produced by a slowly inactivating form of *Shaker*.

K_L channels do not show inactivation during long depolarizing pulses, a feature suggesting that they contribute to the noninactivating component of the macroscopic delayed current. They have a large unitary conductance, 44–55 pS, brief open times, rapid activation, and low voltage activation threshold, and they lack steady-state inactivation. These properties resemble those of K_O channels from embryonic myotubes (Zagotta et al., 1988) and *Shaw* channels from embryonic neurons (Tsunoda and Salkoff, 1995a). Unlike K_O or *Shaw* channels, which appear to contribute very little to the macroscopic current of embryonic myotubes and neuron somata, K_L channels may contribute a significant portion of the delayed macroscopic current of synaptic boutons. This is based on both the relatively large fraction of the noninactivating macroscopic current component and the relatively high occurrence of K_L channels in perforated vesicles.

The high density of voltage-dependent K^+ currents in boutons indicates that these currents exert a strong influence on the excitability of the synaptic membrane. The current density, however, falls short of that reported for neurosecretory boutons from rat posterior pituitary (Bielefeldt et al., 1992). The fast activation kinetics of I_A and I_K suggests that they may contribute to the repolarizing phase of the action potential and thereby regulate peptide release (Thorn et al., 1991). Because of the lack of physiological data, however, it is not yet possible to offer a mechanistic relationship between the physiological activity of type III synaptic boutons and these ionic currents.

Although the functional role of type III boutons is not known, we favor the hypothesis that they regulate the activity of the muscle fibers that they innervate, rather than being involved directly in synaptic transmission or neurosecretion of hormones into the circulating hemolymph. This is suggested by the fact that direct intraterminal stimulation of the boutons does not elicit any obvious postsynaptic current in the muscle fiber. On the other hand, calcium channels were never found in patches of the exposed membrane surface of the bouton, in spite of the presence of a macroscopic calcium current (our unpublished observations). This could be explained by assuming that calcium channels are located in the releasing face of the bouton, as in other presynaptic terminals (Haydon et al., 1994). Should this be the case, it would reinforce the idea that type III boutons secrete into the synaptic space toward the muscle membrane. This possibility raises the question of what is the mechanical role of the muscles that receive type III innervation during larval movement. Additional studies on this bouton will be needed to understand its physiological function and eventually the mechanism of secretion. The use of *ecd*^{1} will be instrumental in this task.

REFERENCES

Anderson MS, Halpern ME, Keshishian H (1988) Identification of the neuropeptide transmitter proctolin in *Drosophila* larvae: characterization of fiber-specific neuromuscular endings. J Neurosci 8:242–255.

Atkinson NS, Robertson GA, Ganetzky B (1991) A component of calcium-activated potassium channels encoded by the *Drosophila slo* locus. Science 253:551–555.

Atwood HL, Govind CK, Wu CF (1993) Differential ultrastructure of synaptic terminals on ventral longitudinal abdominal muscles in *Drosophila* larvae. J Neurobiol 24:1008–1024.

Augustine GJ (1990) Regulation of transmitter release at the squid giant synapse by a presynaptic delayed rectifier potassium current. J Physiol (Lond) 431:343–364.

Baker K, Salkoff L (1990) The *Drosophila Shaker* gene codes for a distinctive K^+ current in a subset of neurons. Neuron 2:129–140.

Baumann A, Krah-Jentgens I, Müller R, Müller-Holtkamp F, Seidel R, Kecskemethy N, Casal J, Ferrús A, Pongs O (1987) Molecular organization of the maternal effect region of the *Shaker* complex of *Drosophila*: characterization of an I_A channel transcript with homology to vertebrate sodium channel. EMBO J 6:3419–3429.

Bennett MK, Scheller RH (1994) A molecular description of synaptic vesicle membrane trafficking. Annu Rev Biochem 63:63–100.

Bielefeldt K, Rotter JL, Jackson MB (1992) Three potassium channels in rat posterior pituitary nerve terminals. J Physiol (Lond) 458:41–67.

Brüggemann A, Pardo LA, Stühmer W, Pongs O (1993) Ether-à-go-go encodes a voltage-gated channel permeable to K^+ and Ca^{2+} and modulated by cAMP. Nature 365:445–448.

Butler A, Wei A, Baker K, Salkoff L (1989) A family of putative potassium channel genes in *Drosophila*. Science 243:943–947.

Byerly L, Leung HT (1988) Ionic currents of *Drosophila* neurons in embryonic cultures. J Neurosci 8:4379–4393.

Canal I, Fariñas I, Gho M, Ferrús A (1994) The presynaptic cell determines the number of synapses in the *Drosophila* optic ganglia. Eur J Neurosci 6:1423–1431.

Chen ML, Hoshi T, Wu CF (1996) Heteromultimeric interactions among K^+ channel subunits from *Shaker* and *eag* families in *Xenopus* oocytes. Neuron 17:535–542.

Chouinard SW, Wilson GF, Schlimgen AK, Ganetzky B (1995) A potassium channel beta subunit related to the aldo-keto reductase superfamily is encoded by the *Drosophila hyperkinetic* locus. Proc Natl Acad Sci USA 92:6763–6767.

Connor JA, Stevens CF (1971a) Inward and delayed outward membrane currents in isolated neural somata under voltage clamp. J Physiol (Lond) 213:1–19.

Connor JA, Stevens CF (1971b) Voltage clamp studies of a transient outward membrane current in gastropod neural somata. J Physiol (Lond) 213:21–30.

Elkins T, Ganetzky B, Wu CF (1986) A *Drosophila* mutation that eliminates a calcium-dependent potassium current. Proc Natl Acad Sci USA 83:8415–8419.

Ferrús A, Llamazares S, de la Pompa JL, Tanouye MA, Pongs O (1990) Genetic analysis of the *Shaker* gene complex of *Drosophila melanogaster*. Genetics 125:383–398.

Forsythe ID (1994) Direct patch recordings from identified presynaptic terminals mediating glutamatergic EPSCs in the rat CNS, *in vitro*. J Physiol (Lond) 479:381–387.

Gardner CC, Kindler S (1996) Synaptic proteins and the assembly of synaptic junctions. Trends Cell Biol 6:429–433.

Garner A, Kauvar L, Lepesant JA (1977) Roles of *ecdysone* in *Drosophila* development. Proc Natl Acad Sci USA 74:5099–5103.

Gho M, Ganetzky B (1992) Analysis of repolarization of presynaptic motor terminals in *Drosophila* larvae using potassium channel-blocking drugs and mutations. J Exp Biol 170:93–111.

Gho M, Mallart A (1986) Two distinct calcium-activated potassium currents in larval muscle fibers of *Drosophila melanogaster*. Pflügers Arch 407:526–533.

Gorczyca MG, Augart C, Budnik V (1993) Insulin-like receptor and

insulin-like peptide are localized at neuromuscular junctions in *Drosophila*. J Neurosci 13:3692–3704.
Haydon PG, Henderson E, Stanley EF (1994) Localization of individual calcium channels at the release face of a presynaptic nerve terminal. Neuron 13:1275–1280.
Horn R, Marty A (1988) Muscarinic activation of ionic currents measured by a new whole-cell recording method. J Gen Physiol 92:145–159.
Isacoff EY, Jan Y-N, Jan LY (1990) Evidence for the formation of heteromultimeric potassium channels in *Xenopus* oocytes. Nature 345:530–534.
Jackson MB (1992) Cable analysis with the whole-cell patch clamp: theory and experiments. Biophys J 61:756–766.
Jahn R, Sudhof TC (1994) Synaptic vesicles and exocytosis. Annu Rev Neurosci 17:219–246.
Jan LY, Jan Y-N (1976) Properties of the larval neuromuscular junction in *Drosophila melanogaster*. J Physiol (Lond) 262:189–214.
Jan LY, Jan Y-N (1992) Structural elements involved in specific K^+ channel functions. Annu Rev Physiol 54:537–555.
Jia X-X, Gorczyca M, Budnik V (1993) Ultrastructure of neuromuscular junctions in *Drosophila*: comparison of wild type and mutants with increase excitability. J Neurobiol 24: 1025–1044.
Johansen J, Halpern ME, Johansen KM, Keshishian H (1989) Stereotypic morphology of glutamatergic synapses on identified muscle cells of *Drosophila* larvae. J Neurosci 9:710–725.
Kamb A, Iverson LE, Tanouye MA (1987) Molecular characterization of *Shaker*, a *Drosophila* gene that encodes a potassium channel. Cell 50:405–413.
Kamb A, Tseng-Crand J, Tanouye MA (1988) Multiple products of the *Drosophila Shaker* gene may contribute to potassium channel diversity. Neuron 1:421–430.
Komatsu A, Singh S, Rathe P, Wu CF (1990) Mutational and gene dosage analysis of calcium-activated potassium channels in *Drosophila*: correlation of micro- and macroscopic currents. Neuron 4:313–321.
Lindsley DL, Zimm GG (1992) The genome of *Drosophila melanogaster*. San Diego: Academic.
Littleton JT, Bellen HJ (1995) Synaptotagmin controls and modulates synaptic-vesicle fusion in a Ca^{2+}-dependent manner. Trends Neurosci 18:177–183.
Llinás R, Steinberg IZ, Walton K (1981) Presynaptic calcium currents in squid giant synapse. Biophys J 33:289–322.
Mallart A, Angaut-Petit D, Bourret-Poulain C, Ferrús A (1991) Nerve terminal excitability and neuromuscular transmission in *T(X;Y)V7* and *Shaker* mutants of *Drosophila melanogaster*. J Neurogenet 7:75–84.
Marty A, Neher E (1983) Tight-seal whole-cell recording. In: Single-channel recording (Sakmann B, Neher E, eds), pp 107–122. New York: Plenum.
Monastirioti M, Gorczyca M, Rapus J, Eckert M, White K, Budnik V (1995) Octopamin immunoreactivity in the fruit fly *Drosophila melanogaster*. J Comp Neurol 356:275–287.
Pongs O (1992) Molecular Biology of voltage-dependent potassium channels. Physiol Rev 72[Suppl 4]:S69–88.
Pongs O, Kecskemethy N, Muller R, Krah-Jentgens I, Baumann A, Kiltz HH, Canal I, Llamazares S, Ferrús A (1988) Shaker encodes a family of putative potassium channel proteins in the nervous system of *Drosophila*. EMBO J 7:1087–1096.
Robitaille R, Garcia ML, Kaczorowski GJ, Charlton MP (1993) Functional colocalization of calcium and calcium-gated potassium channels in control of transmitter release. Neuron 11:645–655.
Rudy B, Kentros C, Weiser M, Fruhling D, Serodio P, Vega-Saenz-de-Miera E, Ellisman MH, Pollock JA, Baker H (1992) Region-specific expression of a K^+ channel gene in brain. Proc Natl Acad Sci USA 89:4603–4607.
Salkoff L (1983) *Drosophila* mutants reveal two components of fast outward current. Nature 302:249–251.
Salkoff L, Wyman R (1981) Genetic modification of potassium channels in *Drosophila Shaker* mutants. Nature 293:228–230.
Schwarz TL (1994) Genetic analysis of neurotransmitter release at the synapse. Curr Opin Neurobiol 4:633–639.
Sheng M, Tsaur M-L, Jan Y-N, Jan LY (1992) Subcellular segregation of two A-type K^+ channel proteins in rat central neurons. Neuron 9:271–284.
Singh S, Wu CF (1989) Complete separation of four potassium currents in *Drosophila*. Neuron 2:1325–1329.
Solc CK, Aldrich RW (1988) Voltage-gated potassium channels in larval CNS neurons of *Drosophila*. J Neurosci 8:2556–2570.
Solc CK, Zagotta WN, Aldrich RW (1987) Single-channel and genetic analyses reveal two distinct A-type potassium channels in *Drosophila*. Science 236:1094–1098.
Stanley EF, Goping G (1991) Characterization of a calcium current in a vertebrate cholinergic presynaptic nerve terminal. J Neurosci 11:985–993.
Tempel BL, Papazian DM, Schwarz TS, Jan YN, Jan LY (1987) Sequence of a probable potassium channel component encoded at *Shaker* locus of *Drosophila*. Science 237:770–775.
Thorn PJ, Wang X, Lemos JR (1991) A fast, transient K^+ current in neurohypophysial nerve terminals of the rat. J Physiol (Lond) 432:313–326.
Tsunoda S, Salkoff L (1995a) Genetic analysis of *Drosophila* neurons: *Shal*, *Shaw*, and *Shab* encode most embryonic potassium currents. J Neurosci 15:1741–1754.
Tsunoda S, Salkoff L (1995b) The major delayed rectifier in both *Drosophila* neurons and muscle is encoded by *Shab*. J Neurosci 15:5209–5221.
Ullrich B, Ushkaryov YA, Sudhof TC (1995) Cartography of neurexins: more than a 1000 isoforms generated by alternative splicing and expressed in distinct subsets of neurons. Neuron 14:497–507.
Veh RW, Lichtinghagen R, Sewing S, Wunder F, Grumbach IM, Pongs O (1995) Immunohistochemical localization of five members of the Kv1 channel subunits: contrasting subcellular locations and neuron-specific co-localizations in rat brain. Eur J Neurosci 7:2189–2205.
Wang JW, Wu CF (1996) In vivo functional role of the *Drosophila hyperkinetic* β subunit in gating and inactivation of *Shaker* K^+ channels. Biophys J 71:3167–3176.
Warmke J, Drysdale R, Ganetzky B (1991) A distinct potassium channel polypeptide encoded by the *Drosophila* eag locus. Science 252:1560–1562.
Wei A, Covarrubias M, Butler A, Baker K, Pak M, Salkoff L (1990) K^+ current diversity is produced by an extended gene family conserved in *Drosophila* and mouse. Science 248:599–603.
Woods DF, Bryant PJ (1991) The disc-large tumor suppressor gene of *Drosophila* encodes a guanylate kinase homolog localized at septate junctions. Cell 66:451–464.
Wu CF, Haugland FN (1985) Voltage clamp analysis of membrane currents in larval muscle fibers of *Drosophila*: alteration of potassium currents in *Shaker* mutants. J Neurosci 5:2626–2640.
Zagotta WN, Brainard MS, Aldrich RW (1988) Single-channel analysis of four distinct classes of potassium channels in *Drosophila* muscle. J Neurosci 8:4765–4779.
Zhong Y, Wu CF (1991) Alteration of four identified K^+ currents in *Drosophila* muscle by mutations in *eag*. Science 252:1562–1564.
Zhong Y, Wu CF (1993) Modulation of different K^+ currents in *Drosophila*: a hypothetical role for the eag subunit in multimeric K^+ channels. J Neurosci 13:4669–4679.